Data report: clay mineral assemblages in cuttings from Hole C0002F, IODP Expedition 338, upper Nankai Trough accretionary prism[1]

Michael B. Underwood[2] and Chen Song[3]

Chapter contents

Abstract

This report summarizes the results of X-ray diffraction analyses of cuttings samples (1–4 mm diameter) from Integrated Ocean Drilling Program Expedition 338 Hole C0002F, located offshore southwest Japan. We analyzed 37 specimens (<2 µm size fraction) from the upper Nankai accretionary prism, collected between 1190 and 1990 meters below seafloor. Smectite is generally the most abundant mineral in the clay-size fraction. Within lithologic Unit IV, smectite in the bulk sediment averages 25.1 wt% (standard deviation = 3.6), whereas illite and kaolinite + chlorite average 18.9 (standard deviation = 2.0) and 11.3 wt% (standard deviation = 2.3), respectively. Within Unit V, smectite in the bulk sediment decreases to an average of 21.8 wt% (standard deviation = 2.8) and values of illite and kaolinite + chlorite average 21.8 (standard deviation = 3.5) and 14.1 wt% (standard deviation = 3.5 and 2.4), respectively. The expandability of illite/smectite averages 69%, and values decrease downhole. The proportion of illite in illite/smectite mixed-layer clays averages 25%, and those values increase downhole. Values of illite crystallinity index (average = $0.52\Delta°2\theta$) are consistent with detrital source areas exposed to advanced levels of diagenesis and anchizone metamorphism.

Introduction

The Nankai Trough region, offshore southwest Japan (Fig. F1), has been sampled by scientific ocean drilling several times over the past four decades (Karig, Ingle, et al., 1975; Kagami, Karig, Coulbourn, et al., 1986; Shipboard Scientific Party, 1991, 2001). The latest drilling efforts are part of the Nankai Trough Seismogenic Zone Experiment (NanTroSEIZE) (Ashi et al., 2009; Screaton et al., 2009; Tobin et al., 2009; Underwood et al., 2010; Expedition 333 Scientists, 2012; also see the "Expedition 338 summary" chapter [Strasser et al., 2014a]). Previous investigators demonstrated that hemipelagic mud(stones) throughout the Nankai region change in composition largely as a function of depositional age (Cook et al., 1975; Chamley, 1980; Chamley et al., 1986; Underwood et al., 1993a, 1993b; Masuda et al., 1996, 2001; Steurer and Underwood, 2003; Underwood and Steurer, 2003; Guo and Underwood, 2012; Underwood and Guo, 2013). As a rule, deposits during the Miocene were enriched in smectite, whereas proportions of detrital illite and chlorite increased steadily during the Pliocene and Quaternary.

[2]Department of Earth and Environmental Science, New Mexico Institute of Mining and Technology, 801 Leroy Place, Socorro New Mexico 87801, USA. UnderwoodM@missouri.edu
[3]Department of Geological Sciences, University of Missouri, 101 Geology Building, Columbia Missouri 65211, USA.

Integrated Ocean Drilling Program (IODP) Site C0002 is located near the seaward edge of Kumano Basin (Fig. F1). IODP Expedition 338 extended Hole C0002F by riser drilling through the upper accretionary prism to 2004 meters below seafloor (mbsf) (see the "Expedition 338 summary" chapter [Strasser et al., 2014a]). The sampled interval contains nannofossils that are Miocene in age (>5.59 Ma). The common lithology is clayey siltstone (hemipelagic mudstone), with variable percentages of medium silt to fine sand (turbidites). A lithologic boundary between Units IV and V occurs at 1740 mbsf, as defined by a sharp reduction of sandstone content (Fig. F2). Stratigraphic details are obscured, however, by drilling technology that placed logging tools between a 12¼ inch drill bit at the base of the bottom-hole assembly and a 20 inch reamer bit above. That configuration of two cutting tools resulted in thorough mixing of cuttings over a vertical interval of at least 43.8 m.

One of the goals of NanTroSEIZE has been to document the abundance and hydration state of clay minerals (especially the smectite group) within accreted Nankai strata. That task is important because of the clay's likely influence on fluid production within the accretionary prism, as well as along the landward-dipping plate interface (e.g., Saffer et al., 2008). This report summarizes the results of X-ray diffraction (XRD) analyses of 37 cuttings samples extracted from Hole C0002F. We focus on common clay minerals (smectite, illite, chlorite, and kaolinite) and on indicators of clay diagenesis.

Methods

Sample preparation

All of the samples analyzed in this study were selected from cuttings measuring 1–4 mm in effective diameter (concentrated by wet sieving). Each extracted interval of cuttings included a companion specimen for shipboard bulk-powder XRD, which provided estimates of the relative abundance of total clay minerals, quartz, feldspar, and calcite (see the "Site C0002" chapter [Strasser et al., 2014b]). Isolation of the clay-size fraction for XRD analyses began with air-drying and gentle hand-crushing of the mudstone with mortar and pestle, after which specimens were immersed in 3% H_2O_2 for at least 24 h to digest organic matter. We added ~250 mL of Na-hexametaphosphate solution (concentration of 4 g/1000 mL distilled H_2O) and inserted the beakers into an ultrasonic bath for several minutes to promote disaggregation and deflocculation. This step (and additional soaking) was repeated until visual inspection

indicated complete disaggregation. Washing consisted of two passes through a centrifuge (8200 revolutions per minute [rpm] for 25 min; ~6000 g) with resuspension in distilled-deionized water after each pass. After transferring the suspended sediment to a 60 mL plastic bottle, each sample was resuspended by vigorous shaking and a 2 min application of a sonic cell probe. The clay-size splits (<2 μm equivalent settling diameter) were then separated by centrifugation (1000 rpm for 2.4 min; ~320 g). Oriented clay aggregates were prepared using the filter-peel method (Moore and Reynolds, 1989) and 0.45 μm membranes. We saturated the clay aggregates with ethylene glycol vapor using a closed vapor chamber heated to 60°C for at least 24 h prior to XRD analysis.

X-ray diffraction

Our analyses of the cuttings samples from Expedition 338 were completed at the New Mexico Bureau of Geology and Mineral Resources using a Panalytical X'Pert Pro diffractometer with Cu anode. Scans of oriented clay aggregates were run at generator settings of 45 kV and 40 mA. The continuous scans cover an angular range of 3° to 26.5°2θ with a scan step time of 1.6 s and step size of 0.01°2θ. Slits were 1.0 (divergence) and 0.1 mm (receiving), and the sample holder was spinning. We processed the digital data using MacDiff software (version 4.2.5) to establish a baseline of intensity, smooth counts, correct peak positions offset by misalignment of the detector (using the quartz [100] peak at 20.95°2θ; d-value = 4.24 Å), and calculate integrated peak areas (total counts). This program also calculated peak width at half height.

Calculations of mineral abundance

The most accurate analytical methods for XRD analyses require calibration with internal standards, use of single-line reference intensity ratios, and some fairly elaborate sample preparation steps to create optimal random particle orientations (e.g., Środoń et al., 2001; Omotoso et al., 2006). Our primary goal throughout the NanTroSEIZE project has been to obtain accurate values for the clay-size fraction from a large suite of samples. To accomplish that goal efficiently, we recorded the integrated areas of a broad smectite (001) peak centered at ~5.3°2θ (d-value = 16.5 Å), the illite (001) peak at ~8.9°2θ (d-value = 9.9 Å), the composite chlorite (002) + kaolinite (001) peak at 12.5°2θ (d-value = 7.06 Å), and the quartz (100) peak at 20.85°2θ (d-value = 4.26 Å). We then applied a matrix of singular value decomposition (SVD) normalization factors (Table T1), calculated af-

ter analyzing standard mineral mixtures (Underwood et al., 2003). Those standards consisted of smectite + illite + chlorite + quartz. The average errors using this method were 3.9% for smectite, 1.0% for illite, 1.9% for chlorite, and 1.6% for quartz. The kaolinite (001) and chlorite (002) reflections overlap almost completely, so we followed a refined version of the Biscaye (1964) method, as documented by Guo and Underwood (2011). The average error of accuracy for the chlorite/kaolinite ratio is 2.6%. To calculate the abundance of individual clay minerals in the bulk mudstone, we multiply each relative percentage value among the clay minerals (where smectite + illite + chlorite + kaolinite = 100%) by the percentage of total clay minerals within the bulk powder (where total clay minerals + quartz + feldspar + calcite = 100%), as determined by shipboard XRD analyses of collocated specimens (see the "Site C0002" chapter [Strasser et al., 2014b]). To facilitate direct comparisons with other published data sets from the region, we also report the weighted peak area percentages for smectite, illite, and chlorite + kaolinite using Biscaye (1965) weighting factors (1 × smectite, 4 × illite, and 2 × chlorite + kaolinite). Errors of accuracy using that method can be substantially greater (±10% or more) as compared to SVD normalization factors (Underwood et al., 2003).

For documentation of clay diagenesis, we utilized the saddle/peak method of Rettke (1981) to calculate percent expandability of smectite and illite/smectite mixed-layer clay. This method is sensitive to the proportions of discrete illite versus illite/smectite mixed-layer clay; we chose the curve for 1:1 mixtures of discrete illite and illite/smectite. A complementary measure of the proportion of illite in the illite/smectite mixed-layer phase considers the center peak position (2θ angle) of the (002/003) peak (following Moore and Reynolds, 1989), using the quartz (100) peak to correct for misalignment of the detector and/ or sample holder. We also report illite crystallinity (Kübler) index as values of peak width at half height (Δ°2θ) for the (001) reflection.

Results

Table T2 shows the peak-area values (total counts) for common minerals in the clay-size fraction, segregated by lithologic unit. We also tabulated the values of mineral abundance (wt%) calculated by SVD normalization factors (Fig. F3) and by Biscaye (1965) peak-area weighting factors (Table T2). The peak intensities for four additional specimens were too low to generate reliable results, so those values were omitted. Relative abundances of clay-size smectite

within Unit IV range from 55 to 30 wt%, with a mean (μ) of 44.3 wt% and a standard deviation (s) of 6.3. Values for illite in the clay-size fraction range from 42 to 29 wt% (μ = 33.4; s = 2.7). Percentages of kaolinite + chlorite in Unit IV range from 26 to 12 wt% (μ = 19.9; s = 3.8); in all cases, chlorite is the dominant mineral over kaolinite. Percentages of clay-size quartz average only 2.5 wt% (s = 2.5). Within Unit V, the clay-size smectite ranges from 44 to 28 wt% (μ = 36.7; s = 6.2). Illite ranges from 55 to 32 wt% (μ = 37.6; s = 4.7), whereas kaolinite + chlorite ranges from 36 to 19 wt% (μ = 23.9; s = 2.6). The average percentage of clay-size quartz is only 1.8 wt%.

Figure F4 illustrates how relative mineral abundances within the bulk sediment change with depth. Bulk sediment smectite values within Unit IV range from 33 to 19 wt% (μ = 25.1; s = 3.6). Those percentages are significantly lower than what Underwood and Guo (2013) documented from coeval (5–6 Ma) Miocene strata at IODP Sites C0011 and C0012 in Shikoku Basin (i.e., the Nankai subduction inputs) (Fig. F1). Illite in the bulk sediment of Unit IV ranges from 25 to 15 wt% (μ = 18.9; s = 2.0), and kaolinite + chlorite ranges from 17 to 7 wt% (μ = 11.3; s = 2.3). Within Unit V, smectite within bulk sediment ranges from 26 to 16 wt% (μ = 21.8; s = 2.8). Illite in the bulk sediment ranges from 27 to 16 wt% (μ = 21.8; s = 3.5), and kaolinite + chlorite ranges from 18 to 11 wt% (μ = 14.1; s = 2.4).

Indicators of clay diagenesis are tabulated in Table T3 and plotted in Figure F5. Illite crystallinity (Kübler) indexes range from 0.67Δ° to 0.41Δ°2θ, with an average value of 0.52Δ°2θ. As a frame of reference, the boundary between advanced diagenesis and anchizone metamorphism is set at 0.52Δ°2θ, and the limit for epizone metamorphism (incipient greenschist facies) is 0.32Δ°2θ (Warr and Mählmann, 2015). The expandability of illite/smectite mixed-layer clays ranges from 89% to 59%, with an average value of 68% (s = 6.9). The proportion of illite in illite/smectite mixed-layer clays ranges from 6% to 49%, with an average value of 25% (s = 8.5). Values are scattered, but we note an increase in the levels of diagenesis with increasing depth (Fig. F5).

Acknowledgments

References

Ashi, J., Lallemant, S., Masago, H., and the Expedition 315 Scientists, 2009. Expedition 315 summary. *In* Kinoshita, M., Tobin, H., Ashi, J., Kimura, G., Lallemant, S., Screaton, E.J., Curewitz, D., Masago, H., Moe, K.T., and the Expedition 314/315/316 Scientists, *Proceedings of the Integrated Ocean Drilling Program,* 314/315/316: Washington, DC (Integrated Ocean Drilling Program Management International, Inc.). http://dx.doi.org/10.2204/iodp.proc.314315316.121.2009

Biscaye, P.E., 1964. Distinction between kaolinite and chlorite in recent sediments by X-ray diffraction. *American Mineralogist,* 49:1281–1289.

Biscaye, P.E., 1965. Mineralogy and sedimentation of recent deep-sea clay in the Atlantic Ocean and adjacent seas and oceans. *Geological Society of America Bulletin,* 76(7):803–831. http://dx.doi.org/10.1130/0016-7606(1965)76[803:MASORD]2.0.CO;2

Chamley, H., 1980. Clay sedimentation and paleoenvironment in the Shikoku Basin since the middle Miocene (Deep Sea Drilling Project Leg 58, North Philippine Sea). *In* Klein, G. de V., Kobayashi, K., et al., *Initial Reports of the Deep Sea Drilling Project,* 58: Washington, DC (U.S. Govt. Printing Office), 669–678. http://dx.doi.org/10.2973/dsdp.proc.58.118.1980

Chamley, H., Cadet, J.-P., and Charvet, J., 1986. Nankai Trough and Japan Trench late Cenozoic paleoenvironments deduced from clay mineralogic data. *In* Kagami, H., Karig, D.E., Coulbourn, W.T., et al., *Initial Reports of the Deep Sea Drilling Project,* 87: Washington, DC (U.S. Govt. Printing Office), 633–641. http://dx.doi.org/10.2973/dsdp.proc.87.113.1986

Cook, H.E., Zemmels, I., and Matti, J.C., 1975. X-ray mineralogy data, far western Pacific, Leg 31 Deep Sea Drilling Project. *In* Karig, D.E., Ingle, J.C., Jr., et al., *Initial Reports of the Deep Sea Drilling Project,* 31: Washington (U.S. Govt. Printing Office), 883–895. http://dx.doi.org/10.2973/dsdp.proc.31.app.1975

Expedition 333 Scientists, 2012. Expedition 333 summary. *In* Henry, P., Kanamatsu, T., Moe, K., and the Expedition 333 Scientists, *Proceedings of the Integrated Ocean Drilling Program,* 333: Tokyo (Integrated Ocean Drilling Program Management International, Inc.). http://dx.doi.org/10.2204/iodp.proc.333.101.2012

Guo, J., and Underwood, M.B., 2011. Data report: refined method for calculating percentages of kaolinite and chlorite from X-ray diffraction data, with application to the Nankai margin of southwest Japan. *In* Kinoshita, M., Tobin, H., Ashi, J., Kimura, G., Lallemant, S., Screaton, E.J., Curewitz, D., Masago, H., Moe, K.T., and the Expedition 314/315/316 Scientists, *Proceedings of the Integrated Ocean Drilling Program,* 314/315/316: Washington, DC (Integrated Ocean Drilling Program Management International, Inc.). http://dx.doi.org/10.2204/iodp.proc.314315316.201.2011

Guo, J., and Underwood, M.B., 2012. Data report: clay mineral assemblages from the Nankai Trough accretionary prism and the Kumano Basin, IODP Expeditions 315 and 316, NanTroSEIZE Stage 1. *In* Kinoshita, M., Tobin, H., Ashi, J., Kimura, G., Lallemant, S., Screaton, E.J., Curewitz, D., Masago, H., Moe, K.T., and the Expedition 314/315/316 Scientists, *Proceedings of the Integrated Ocean Drilling Program,* 314/315/316: Washington, DC (Integrated Ocean Drilling Program Management International, Inc.). http://dx.doi.org/10.2204/iodp.proc.314315316.202.2012

Kagami, H., Karig, D.E., Coulbourn, W.T., et al., 1986. *Initial Reports of the Deep Sea Drilling Project,* 87: Washington, DC (U.S. Govt. Printing Office). http://dx.doi.org/10.2973/dsdp.proc.87.1986

Karig, D.E., Ingle, J.C., Jr., et al., 1975. *Initial Reports of the Deep Sea Drilling Project,* 31: Washington, DC (U.S. Govt. Printing Office). http://dx.doi.org/10.2973/dsdp.proc.31.1975

Masuda, H., O'Neil, J.R., Jiang, W.-T., and Peacor, D.R., 1996. Relation between interlayer composition of authigenic smectite, mineral assemblages, I/S reaction rate and fluid composition in silicic ash of the Nankai Trough. *Clays and Clay Minerals,* 44(4):443–459. http://dx.doi.org/10.1346/CCMN.1996.0440402

Masuda, H., Peacor, D.R., and Dong, H., 2001. Transmission electron microscopy study of conversion of smectite to illite in mudstones of the Nankai Trough: contrast with coeval bentonites. *Clays and Clay Minerals,* 49(2):109–118. http://dx.doi.org/10.1346/CCMN.2001.0490201

Moore, D.M., and Reynolds, R.C., Jr., 1989. Quantitative analysis. *In* Moore, D.M., and Reynolds, R.C., Jr. (Eds.), *X-Ray Diffraction and the Identification and Analysis of Clay Minerals:* New York (Oxford Univ. Press USA), 272–309.

Omotoso, O., McCarty, D.K., Hillier, S., and Kleeberg, R., 2006. Some successful approaches to quantitative mineral analysis as revealed by the 3rd Reynolds Cup contest. *Clays and Clay Minerals,* 54(6):748–760. http://dx.doi.org/10.1346/CCMN.2006.0540609

Rettke, R.C., 1981. Probable burial diagenetic and provenance effects on Dakota Group clay mineralogy, Denver Basin. *Journal of Sedimentary Petrology,* 51(2):541–551. http://dx.doi.org/10.1306/212F7CCF-2B24-11D7-8648000102C1865D

Saffer, D.M., Underwood, M.B., and McKiernan, A.W., 2008. Evaluation of factors controlling smectite transformation and fluid production in subduction zones: application to the Nankai Trough. *Island Arc,* 17(2):208–230. http://dx.doi.org/10.1111/j.1440-1738.2008.00614.x

Screaton, E.J., Kimura, G., Curewitz, D., and the Expedition 316 Scientists, 2009. Expedition 316 summary. *In* Kinoshita, M., Tobin, H., Ashi, J., Kimura, G., Lallemant, S., Screaton, E.J., Curewitz, D., Masago, H., Moe, K.T., and the Expedition 314/315/316 Scientists, *Pro-*

ceedings of the Integrated Ocean Drilling Program, 314/315/316: Washington, DC (Integrated Ocean Drilling Program Management International, Inc.). http://dx.doi.org/10.2204/iodp.proc.314315316.131.2009

Shipboard Scientific Party, 1991. Site 808. In Taira, A., Hill, I., Firth, J.V., et al., Proceedings of the Ocean Drilling Program, Initial Reports, 131: College Station, TX (Ocean Drilling Program), 71–269. http://dx.doi.org/10.2973/odp.proc.ir.131.106.1991

Shipboard Scientific Party, 2001. Leg 190 summary. In Moore, G.F., Taira, A., Klaus, A., et al., Proceedings of the Ocean Drilling Program, Initial Reports, 190: College Station, TX (Ocean Drilling Program), 1–87. http://dx.doi.org/10.2973/odp.proc.ir.190.101.2001

Środoń, J., Drits, V.A., McCarty, D.K., Hsieh, J.C.C., and Eberl, D.D., 2001. Quantitative X-ray diffraction analysis of clay-bearing rocks from random preparations. Clays and Clay Minerals, 49(6):514–528. http://ccm.geoscienceworld.org/cgi/content/abstract/49/6/514

Steurer, J.F., and Underwood, M.B., 2003. Clay mineralogy of mudstones from the Nankai Trough reference Sites 1173 and 1177 and frontal accretionary prism Site 1174. In Mikada, H., Moore, G.F., Taira, A., Becker, K., Moore, J.C., and Klaus, A. (Eds.), Proceedings of the Ocean Drilling Program, Scientific Results, 190/196: College Station, TX (Ocean Drilling Program), 1–37. http://dx.doi.org/10.2973/odp.proc.sr.190196.211.2003

Strasser, M., Dugan, B., Kanagawa, K., Moore, G.F., Toczko, S., Maeda, L., Kido, Y., Moe, K.T., Sanada, Y., Esteban, L., Fabbri, O., Geersen, J., Hammerschmidt, S., Hayashi, H., Heirman, K., Hüpers, A., Jurado Rodriguez, M.J., Kameo, K., Kanamatsu, T., Kitajima, H., Masuda, H., Milliken, K., Mishra, R., Motoyama, I., Olcott, K., Oohashi, K., Pickering, K.T., Ramirez, S.G., Rashid, H., Sawyer, D., Schleicher, A., Shan, Y., Skarbek, R., Song, I., Takeshita, T., Toki, T., Tudge, J., Webb, S., Wilson, D.J., Wu, H.-Y., and Yamaguchi, A., 2014a. Expedition 338 summary. In Strasser, M., Dugan, B., Kanagawa, K., Moore, G.F., Toczko, S., Maeda, L., and the Expedition 338 Scientists, Proceedings of the Integrated Ocean Drilling Program, 338: Yokohama (Integrated Ocean Drilling Program). http://dx.doi.org/10.2204/iodp.proc.338.101.2014

Strasser, M., Dugan, B., Kanagawa, K., Moore, G.F., Toczko, S., Maeda, L., Kido, Y., Moe, K.T., Sanada, Y., Esteban, L., Fabbri, O., Geersen, J., Hammerschmidt, S., Hayashi, H., Heirman, K., Hüpers, A., Jurado Rodriguez, M.J., Kameo, K., Kanamatsu, T., Kitajima, H., Masuda, H., Milliken, K., Mishra, R., Motoyama, I., Olcott, K., Oohashi, K., Pickering, K.T., Ramirez, S.G., Rashid, H., Sawyer, D., Schleicher, A., Shan, Y., Skarbek, R., Song, I., Takeshita, T., Toki, T., Tudge, J., Webb, S., Wilson, D.J., Wu, H.-Y., and Yamaguchi, A., 2014b. Site C0002. In Strasser, M., Dugan, B., Kanagawa, K., Moore, G.F., Toczko, S., Maeda, L., and the Expedition 338 Scientists, Proceedings of the Integrated Ocean Drilling Program, 338: Yokohama (Integrated Ocean Drilling Program). http://dx.doi.org/10.2204/iodp.proc.338.103.2014

Tobin, H., Kinoshita, M., Ashi, J., Lallemant, S., Kimura, G., Screaton, E.J., Moe, K.T., Masago, H., Curewitz, D., and the Expedition 314/315/316 Scientists, 2009. NanTroSEIZE Stage 1 expeditions: introduction and synthesis of key results. In Kinoshita, M., Tobin, H., Ashi, J., Kimura, G., Lallemant, S., Screaton, E.J., Curewitz, D., Masago, H., Moe, K.T., and the Expedition 314/315/316 Scientists, Proceedings of the Integrated Ocean Drilling Program, 314/315/316: Washington, DC (Integrated Ocean Drilling Program Management International, Inc.). http://dx.doi.org/10.2204/iodp.proc.314315316.101.2009

Underwood, M.B., Basu, N., Steurer, J., and Udas, S., 2003. Data report: normalization factors for semiquantitative X-ray diffraction analysis, with application to DSDP Site 297, Shikoku Basin. In Mikada, H., Moore, G.F., Taira, A., Becker, K., Moore, J.C., and Klaus, A. (Eds.), Proceedings of the Ocean Drilling Program, Scientific Results, 190/196: College Station, TX (Ocean Drilling Program), 1–28. http://dx.doi.org/10.2973/odp.proc.sr.190196.203.2003

Underwood, M.B., and Guo, J., 2013. Data report: clay mineral assemblages in the Shikoku Basin, NanTroSEIZE subduction inputs, IODP Sites C0011 and C0012. In Saito, S., Underwood, M.B., Kubo, Y., and the Expedition 322 Scientists, Proceedings of the Integrated Ocean Drilling Program, 322: Tokyo (Integrated Ocean Drilling Program Management International, Inc.). http://dx.doi.org/10.2204/iodp.proc.322.202.2013

Underwood, M.B., Orr, R., Pickering, K., and Taira, A., 1993a. Provenance and dispersal patterns of sediments in the turbidite wedge of Nankai Trough. In Hill, I.A., Taira, A., Firth, J.V., et al., Proceedings of the Ocean Drilling Program, Scientific Results, 131: College Station, TX (Ocean Drilling Program), 15–34. http://dx.doi.org/10.2973/odp.proc.sr.131.105.1993

Underwood, M.B., Pickering, K., Gieskes, J.M., Kastner, M., and Orr, R., 1993b. Sediment geochemistry, clay mineralogy, and diagenesis: a synthesis of data from Leg 131, Nankai Trough. In Hill, I.A., Taira, A., Firth, J.V., et al., Proceedings of the Ocean Drilling Program, Scientific Results, 131: College Station, TX (Ocean Drilling Program), 343–363. http://dx.doi.org/10.2973/odp.proc.sr.131.137.1993

Underwood, M.B., Saito, S., Kubo, Y., and the Expedition 322 Scientists, 2010. Expedition 322 summary. In Saito, S., Underwood, M.B., Kubo, Y., and the Expedition 322 Scientists, Proceedings of the Integrated Ocean Drilling Program, 322: Tokyo (Integrated Ocean Drilling Program Management International, Inc.). http://dx.doi.org/10.2204/iodp.proc.322.101.2010

Underwood, M.B., and Steurer, J.F., 2003. Composition and sources of clay from the trench slope and shallow accretionary prism of Nankai Trough. In Mikada, H., Moore, G.F., Taira, A., Becker, K., Moore, J.C., and Klaus, A. (Eds.), Proceedings of the Ocean Drilling Program, Scientific Results, 190/196: College Station, TX (Ocean Drilling Program), 1–28. http://dx.doi.org/10.2973/odp.proc.sr.190196.206.2003

Warr, L.N., and Mählmann, R.F., 2015. Recommendations for Kübler Index standardization. *Clay Minerals*, 50(3):283–286. http://dx.doi.org/10.1180/claymin.2015.050.3.02

Figure F1. Map of the Nankai Trough and Kumano Basin study area (NanTroSEIZE transect) with locations of Sites C0002, C0011, and C0012. The composition of sediment at Site C0002 is compared to coeval (late Miocene) deposits at Sites C0011 and C0012.
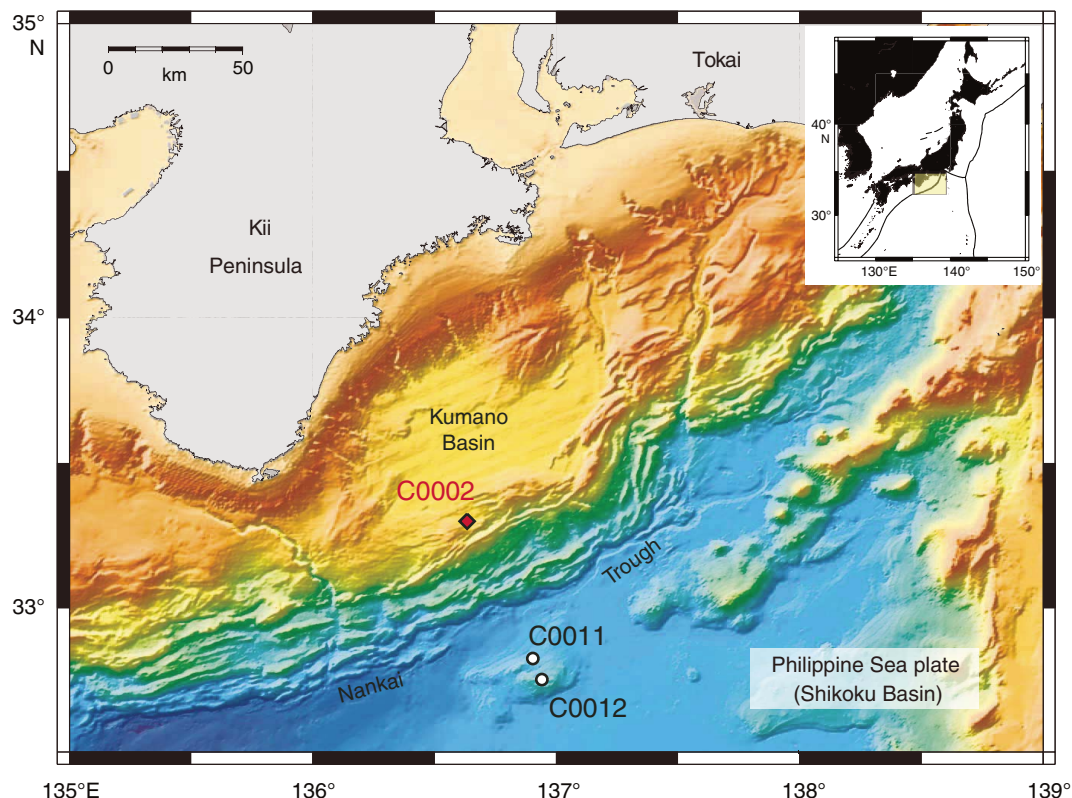
Figure F2. Seismic in-line section crossing Kumano Basin showing location of Site C0002 and lithologic units defined by shipboard analyses of cores and cuttings (see the "Expedition 338 summary" chapter [Strasser et al., 2014a]). LWD = logging while drilling, VE = vertical exaggeration.
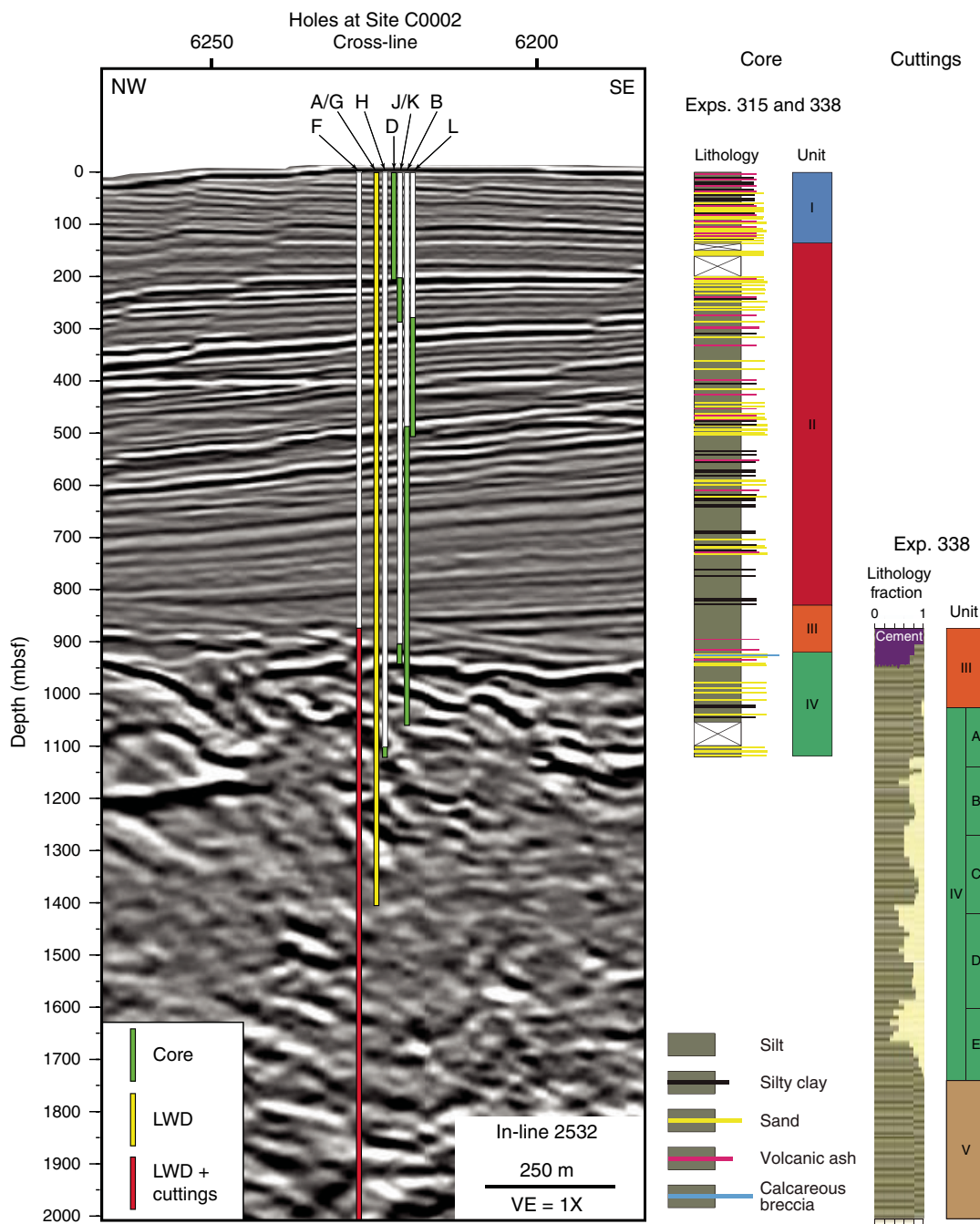
Figure F3. Calculated abundance (relative wt%) of smectite, illite, chlorite, kaolinite, and quartz within the clay-size fraction of cuttings (1–4 mm) from Hole C0002F. Stratigraphic summary is from the **"Expedition 338 summary"** chapter (Strasser et al., 2014a).
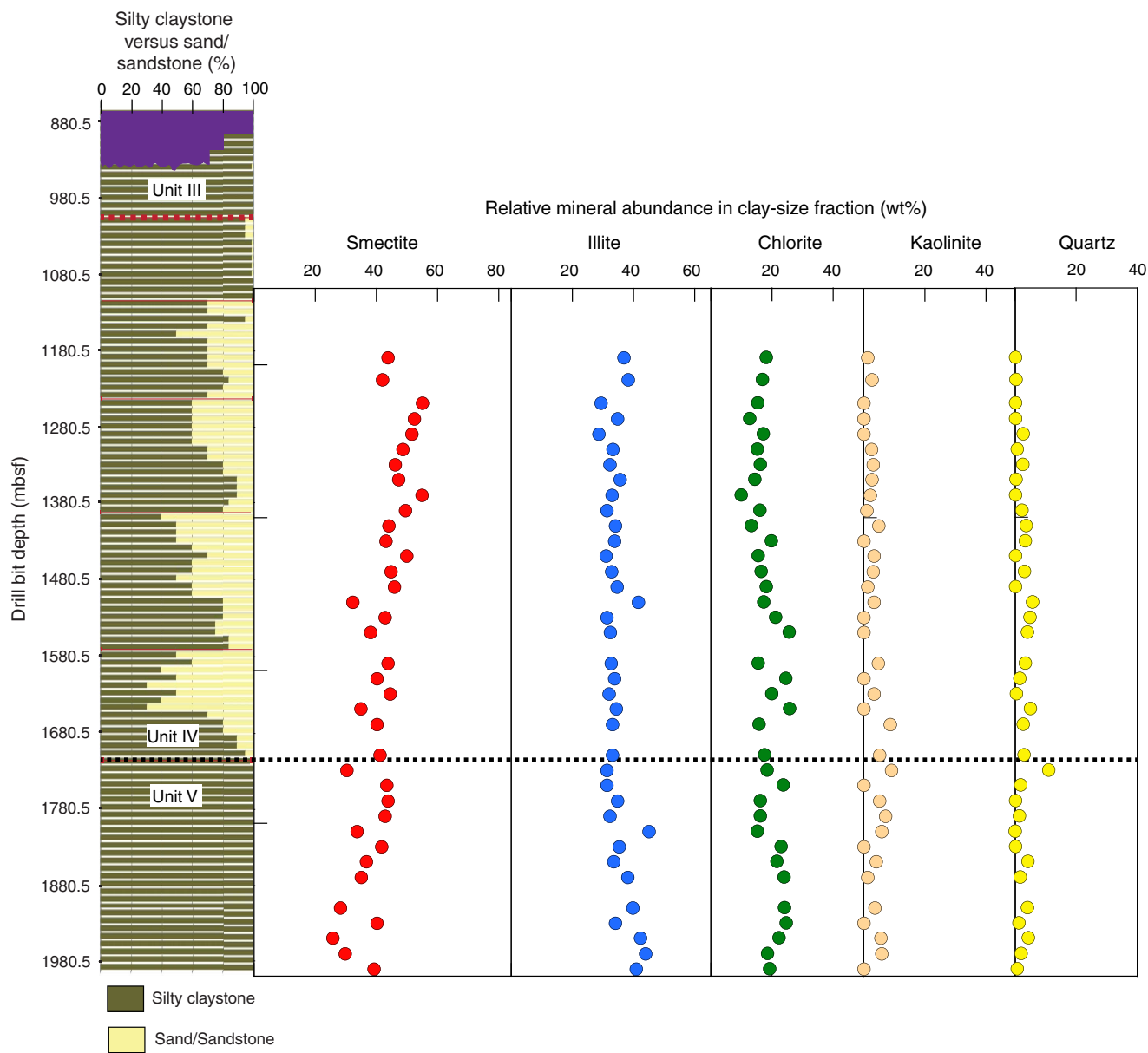
Figure F4. Calculated abundances (relative wt%) of total clay minerals, smectite, illite, and chlorite + kaolinite within bulk sediment cuttings (1–4 mm) from Hole C0002F. Stratigraphic summary is from the **"Expedition 338 summary"** chapter (Strasser et al., 2014a).
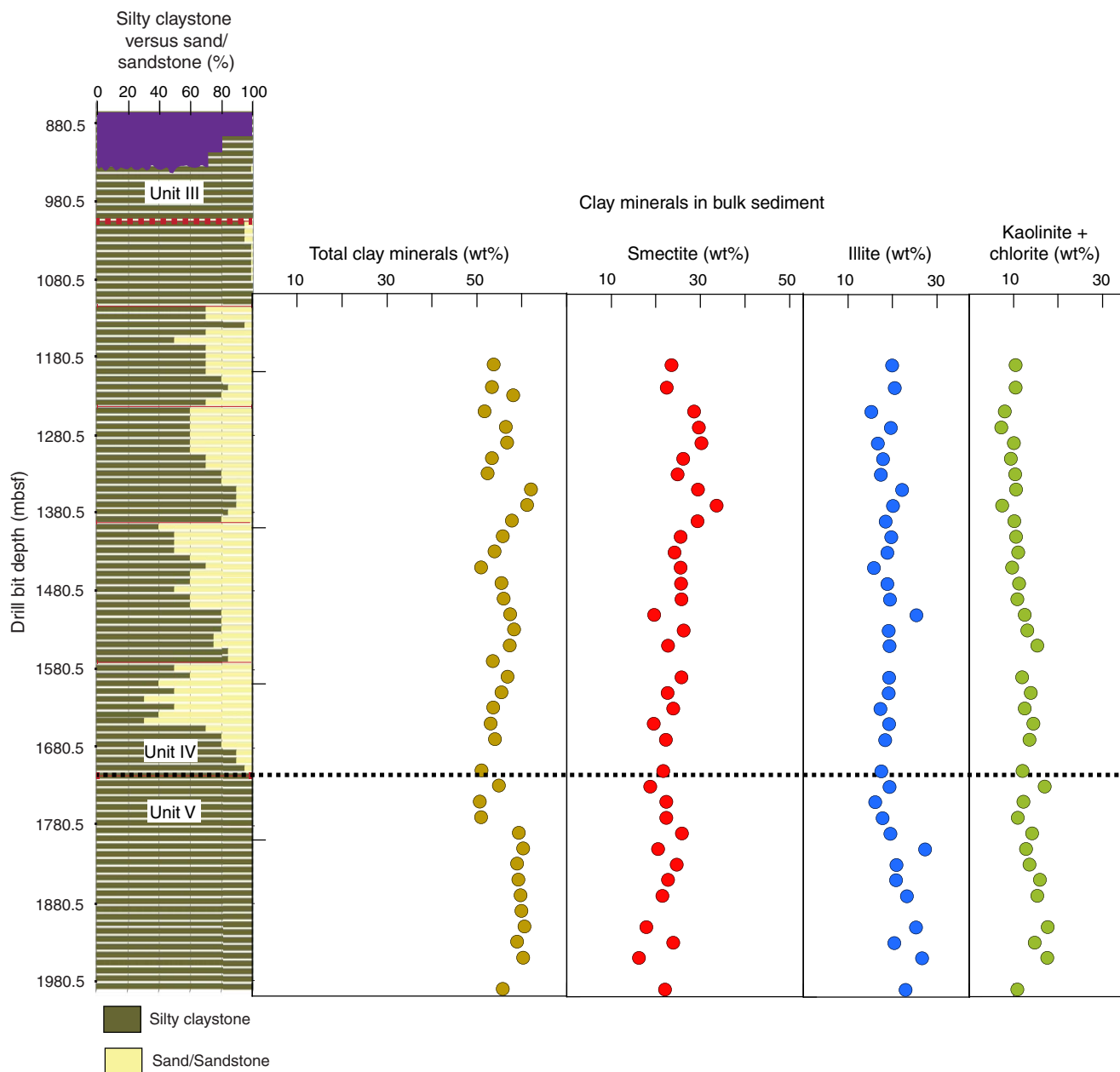
Figure F5. Illite/smectite (I/S) expandability, illite abundance in I/S mixed-layer clay, and illite crystallinity index within the clay-size fraction of cuttings (1–4 mm) from Hole C0002F. Dashed trend lines are qualitative.
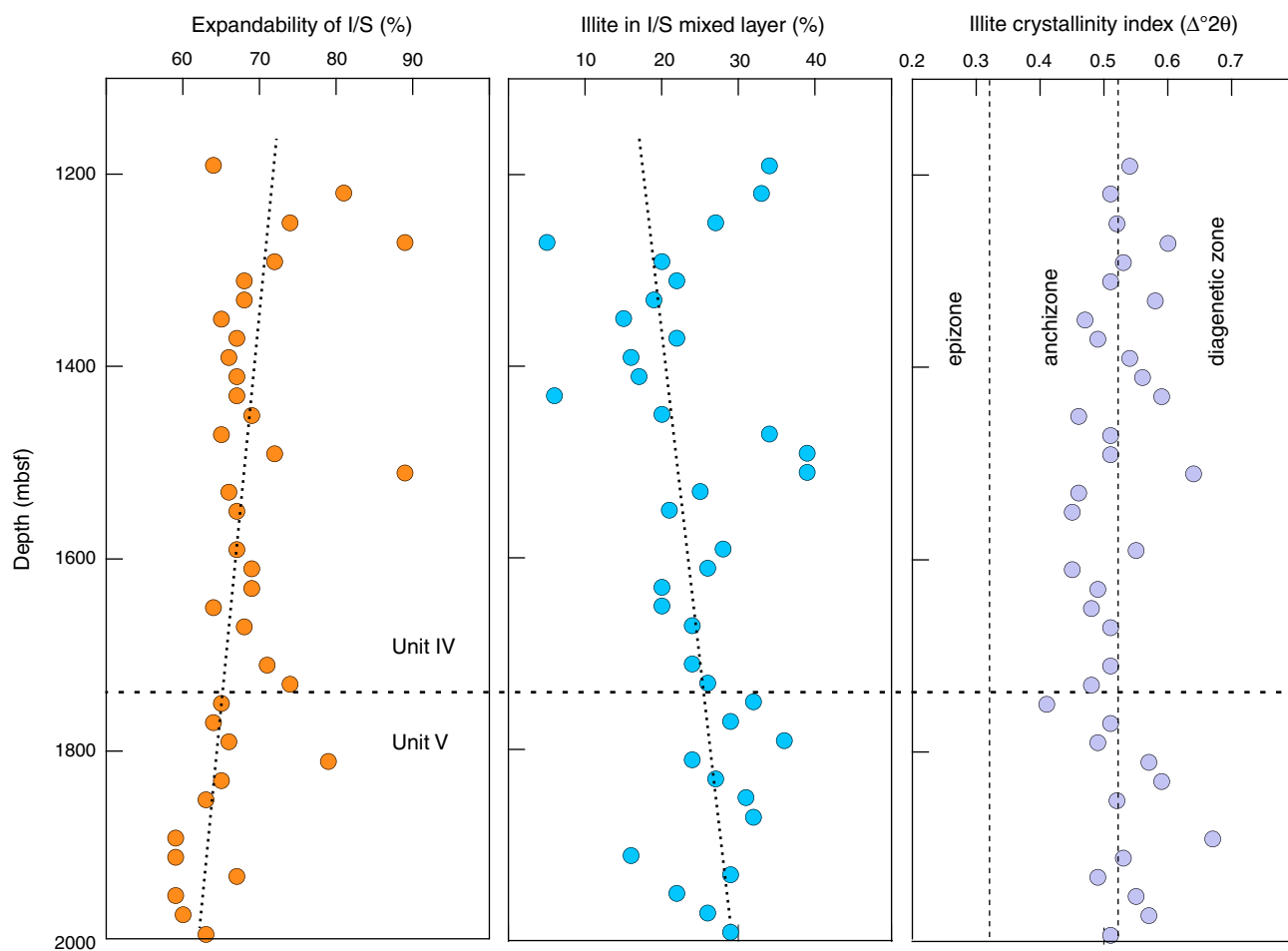
Table T1. Matrix of normalization factors derived from singular value decomposition and used to calculate relative mineral abundances in clay-size aggregates, Hole C0002F.

Influencing mineral	Target mineral in standard mixture			
	Smectite	Illite	Chlorite	Quartz
Smectite	7.4475294E–04	–3.1953641E–05	–7.5067212E–05	–1.5661915E–04
Illite	6.3114654E–05	3.7866938E–03	8.4222964E–05	1.1769286E–04
Chlorite	–3.5636057E–04	–6.7378140E–05	2.5121504E–03	5.2290707E–05
Quartz	9.3573136E–03	3.6491468E–03	3.2755411E–03	1.4825645E–02

Table T2. Results of X-ray diffraction analyses (<2 µm size fraction) for cuttings samples (1–4 mm), Hole C0002F.

| Cuttings interval | Depth (mbsf) | Integrated peak area (total counts) | | | | | | Relative abundance in clay-size fraction | | | | | | | | | Relative abundance in bulk sediment (wt%) | | | |
| | | Smectite (001) | Illite (001) | Kaolinite (001) + chlorite (002) | Quartz (100) | Kaolinite (002) + chlorite (004) | Half peak chlorite (004) | SVD normalization factors (wt%) | | | | | | Biscaye factors (%)* | | | | | | |
								Smectite	Illite	Kaolinite + chlorite	Quartz	Kaolinite	Chlorite	Smectite	Illite	Kaolinite + chlorite	Total clay minerals	Smectite	Illite	Kaolinite + chlorite
338-C0002F- Unit IV																				
82	1190.5	26424	4669	3978	220	2778	1328	43.7	36.8	19.3	0.2	1.2	18.1	50	35	15	53.7	23.5	19.8	10.4
86	1219.5	21392	4066	3336	166	2593	1170	42.0	38.3	19.4	0.3	2.7	16.8	48	37	15	53.3	22.4	20.5	10.4
96	1250.5	32558	3696	3372	271	2588	1292	55.1	29.3	15.4	0.2	0.0	15.4	60	27	12	51.7	28.5	15.2	8.0
100	1270.5	32249	4574	2936	269	1895	969	52.4	34.7	12.7	0.2	0.0	12.7	57	32	10	56.4	29.6	19.6	7.2
104	1290.5	27847	3325	3306	338	2335	1176	51.6	28.6	17.1	2.7	0.0	17.1	58	28	14	56.7	30.1	16.7	10.0
108	1310.5	31030	4522	3948	301	3007	1352	48.6	33.2	17.5	0.7	2.5	15.1	54	32	14	53.3	26.1	17.8	9.4
112	1330.5	29404	4388	4236	347	3276	1451	46.2	32.2	19.2	2.5	3.1	16.1	53	32	15	52.4	24.8	17.3	10.3
116	1350.5	29158	4662	3662	268	2615	1163	47.3	35.6	16.9	0.3	2.6	14.3	53	34	13	62.0	29.4	22.1	10.5
122	1370.5	43842	5547	3830	182	2341	1016	54.8	32.9	12.2	0.2	2.2	9.9	59	30	10	61.1	33.5	20.1	7.4
126	1390.5	24769	3354	3035	287	2420	1159	49.5	31.2	17.1	2.3	1.0	16.0	56	30	14	57.8	29.3	18.4	10.1
132	1410.5	32564	5447	4640	435	3580	1443	44.1	34.1	18.1	3.6	4.8	13.3	51	34	15	55.7	25.5	19.7	10.5
136	1430.5	33448	5642	5242	438	3650	1941	43.1	33.8	19.7	3.4	0.0	19.7	50	34	16	53.9	24.1	18.8	11.0
140	1450.5	30385	3987	4027	245	2628	1147	49.9	31.0	18.9	0.2	3.3	15.5	56	29	15	50.9	25.5	15.8	9.6
144	1470.5	28486	4489	4287	359	2625	1165	44.7	32.8	19.5	3.1	3.1	16.4	52	33	16	55.5	25.6	18.8	11.2
150	1490.5	33565	5283	4854	232	3971	1895	45.9	34.6	19.4	0.2	1.3	18.1	52	33	15	55.9	25.7	19.4	10.8
155	1510.5	21361	6122	4548	380	2776	1228	32.2	41.6	20.4	5.7	3.3	17.2	39	45	17	57.4	19.6	25.3	12.5
161	1530.5	24835	3923	4212	373	3131	1668	42.8	31.2	21.2	4.8	0.0	21.2	51	32	17	58.3	26.2	19.1	13.0
167	1550.5	20722	3741	4596	291	3404	1927	38.1	32.4	25.6	4.0	0.0	25.6	46	33	20	57.3	22.7	19.3	15.3
177	1590.5	31102	4989	4917	403	4126	1713	43.8	32.7	20.2	3.3	4.7	15.5	51	33	16	56.8	25.7	19.2	11.9
184	1610.5	34264	6039	6879	361	5168	2853	40.1	33.8	24.5	1.6	0.0	24.5	47	33	19	55.5	22.6	19.1	13.8
189	1630.5	40236	6066	7011	369	4785	2149	44.5	32.0	23.2	0.4	3.3	19.9	51	31	18	53.6	23.9	17.2	12.5
195	1650.5	25257	5316	6153	402	4537	2443	34.9	34.3	25.8	5.0	0.0	25.8	43	36	21	53.1	19.5	19.2	14.4
201	1670.5	29727	5171	5965	354	3919	1444	40.1	33.1	24.3	2.6	8.6	15.7	48	33	19	54.0	22.2	18.3	13.5
209	1710.5	36947	6335	6865	465	5017	2095	41.1	33.1	22.8	3.0	5.2	17.6	49	33	18	51.0	21.6	17.4	12.0
213	1730.5	10640	2532	3371	323	2944	1116	30.3	31.2	27.4	11.0	9.0	18.4	39	37	25	54.9	18.7	19.3	16.9
						Mean:		44.3	33.4	19.9	2.5	2.5	17.4	51	33	16	55.3	25.1	18.9	11.3
						Standard deviation:		6.3	2.7	3.8	2.5	2.5	3.8	5	4	3	2.8	3.6	2.0	2.3
Unit V																				
217	1750.5	25195	3829	4586	274	3048	1675	43.4	31.3	23.6	1.8	0.0	23.6	51	31	18	50.6	22.3	16.1	12.2
223	1770.5	30331	4954	4963	175	3161	1301	43.7	34.7	21.4	0.2	5.2	16.2	50	33	17	50.9	22.3	17.7	10.9
229	1790.5	29102	4615	5295	307	3107	1205	42.8	32.3	23.3	1.5	7.1	16.2	50	32	18	59.3	25.8	19.5	14.1
233	1810.5	35576	9648	7113	243	4948	1968	33.7	45.0	21.1	0.1	5.9	15.2	40	44	16	60.3	20.4	27.2	12.8
238	1830.5	34256	5943	6164	222	4229	2209	41.7	35.3	22.9	0.2	0.0	22.9	49	34	18	58.9	24.6	20.8	13.5
250	1850.5	31783	6159	7322	459	5323	2360	36.7	33.5	25.7	4.2	4.1	21.6	45	35	21	59.2	22.7	20.7	15.9
255	1870.5	30565	6861	7022	321	4976	2399	35.1	38.1	25.1	1.7	1.3	23.9	42	38	19	59.9	21.4	23.2	15.3
265	1910.5	22623	6675	7039	339	4407	1993	28.2	39.8	27.8	4.1	3.7	24.1	36	42	22	60.6	17.8	25.2	17.6

Table T2 (continued).

Cuttings interval	Depth (mbsf)	Integrated peak area (total counts)						Relative abundance in clay-size fraction									Relative abundance in bulk sediment (wt%)			
								SVD normalization factors (wt%)						Biscaye factors (%)*						
		Smectite (001)	Illite (001)	Kaolinite (001) + chlorite (002)	Quartz (100)	Kaolinite (002) + chlorite (004)	Half peak chlorite (004)	Smectite	Illite	Kaolinite + chlorite	Quartz	Kaolinite	Chlorite	Smectite	Illite	Kaolinite + chlorite	Total clay minerals	Smectite	Illite	Kaolinite + chlorite
269	1930.5	36045	6383	7246	367	5464	2954	40.1	34.0	24.6	1.3	0.0	24.6	47	34	19	58.9	23.9	20.3	14.7
274	1950.5	22607	7738	7643	351	5333	2285	25.7	42.2	27.8	4.3	5.5	22.3	33	45	22	60.3	16.2	26.6	17.5
282	1970.5	27965	8532	7220	299	4353	1797	29.7	44.0	24.4	2.0	5.9	18.5	37	45	19	No bulk powder data			
286	1990.5	34013	7448	5572	315	3178	1661	39.2	40.9	19.2	0.7	0.0	19.2	45	40	15	55.7	22.0	22.9	10.8
							Mean:	36.7	37.6	23.9	1.8	3.2	20.7	44	38	19	57.7	21.8	21.8	14.1
							Standard deviation:	6.2	4.7	2.6	1.6	2.8	3.5	6	5	2	3.7	2.8	3.5	2.4

* = Biscaye (1965) peak area weighting factors are 1 × smecite, 4 × illite, and 2 × chlorite + kaolinite. SVD = singular value decomposition.

Table T3. Illite/smectite expandability values, illite abundance in illite/smectite (I/S) mixed-layer clay (<2 µm size fraction), and illite crystallinity index for cuttings samples (1–4 mm), Hole C0002F.

Cuttings interval (cm)	Depth (mbsf)	S(001) saddle (cps)	S(001) peak (cps)	Saddle:peak ratio	Expandability (%)	I(002) + S(003) (°2θ)	Illite in I/S (%)	Crystallinity index (Δ°2θ)
338-C0002F-								
82	1190.5	213	319	0.67	64	16.05	34	0.54
86	1219.5	56	173	0.32	81	16.04	33	0.51
96	1250.5	132	294	0.45	74	15.97	27	0.52
100	1270.5	50	240	0.21	89	15.74	5	0.60
104	1290.5	125	264	0.47	72	15.89	20	0.53
108	1310.5	190	342	0.56	68	15.91	22	0.51
112	1330.5	212	371	0.57	68	15.88	19	0.58
116	1350.5	235	373	0.63	65	15.84	15	0.47
122	1370.5	303	511	0.59	67	15.91	22	0.49
126	1390.5	182	303	0.60	66	15.85	16	0.54
132	1410.5	232	398	0.58	67	15.86	17	0.56
136	1430.5	243	417	0.58	67	15.75	6	0.59
140	1450.5	200	370	0.54	69	15.89	20	0.46
144	1470.5	221	351	0.63	65	16.05	34	0.51
150	1490.5	159	332	0.48	72	16.12	39	0.51
155	1510.5	32	160	0.20	89	16.12	39	0.64
161	1530.5	189	314	0.60	66	15.95	25	0.46
167	1550.5	160	275	0.58	67	15.90	21	0.45
177	1590.5	208	356	0.58	67	15.98	28	0.55
184	1610.5	188	352	0.53	69	15.96	26	0.45
189	1630.5	252	466	0.54	69	15.89	20	0.49
195	1650.5	215	324	0.66	64	15.89	20	0.48
201	1670.5	200	360	0.56	68	15.94	24	0.51
209	1710.5	180	360	0.50	71	15.93	24	0.51
213	1730.5	50	112	0.45	74	15.96	26	0.48
217	1750.5	197	316	0.62	65	16.03	32	0.41
223	1770.5	237	365	0.65	64	15.99	29	0.51
229	1790.5	220	356	0.62	66	16.09	36	0.49
233	1810.5	90	254	0.35	79	15.94	24	0.57
238	1830.5	252	397	0.63	65	15.97	27	0.59
250	1850.5	256	393	0.65	64	16.02	31	0.52
255	1870.5	286	413	0.69	63	16.03	32	0.53
265	1910.5	272	352	0.77	59	15.85	16	0.53
269	1930.5	247	429	0.58	67	15.99	29	0.49
274	1950.5	281	364	0.77	59	15.91	22	0.55
282	1970.5	295	396	0.74	60	15.96	26	0.57
286	1990.5	280	413	0.68	63	15.99	29	0.51
				Mean:	69		25	0.52
				Standard deviation:	6.8		7.8	0.05

cps = counts per step.